24. M. Grace *et al.*, *J. Phys. B* **40**, S103 (2007).
25. T. Hansson, *Phys. Rev. A* **61**, 033404 (2000).
26. F. A. Bovino *et al.*, *Phys. Rev. Lett.* **95**, 240407 (2005).
27. T. J. Dunn, I. A. Walmsley, S. Mukamel, *Phys. Rev. Lett.* **74**, 884 (1995).
28. T. J. Dunn, J. N. Sweetser, I. A. Walmsley, C. Radzewicz, *Phys. Rev. Lett.* **70**, 3388 (1993).
29. C. Brif, H. Rabitz, S. Wallentowitz, I. A. Walmsley, *Phys. Rev. A* **63**, 063404 (2001).
30. S. Wallentowitz, I. A. Walmsley, L. J. Waxer, Th. Richter, *J. Phys. B* **35**, 1967 (2002).
31. A. J. Ross, P. Crozet, C. Effantin, J. D'Incan, R. F. Barrow, *J. Phys. B* **20**, 6225 (1987).
32. I. A. Walmsley, L. Waxer, *J. Phys. B.* **31**, 1825 (1998).
33. C. Iaconis, I. A. Walmsley, *Opt. Lett.* **23**, 792 (1998).
34. J. Janszky, A. V. Vinogradov, I. A. Walmsley, J. Mostowski, *Phys. Rev. A* **50**, 732 (1994).

35. This work was supported by the Defense Advanced Research Projects Agency (DARPA) QuIST. I.A.W. acknowledges support by the UK Quantum Information Processing Interdisciplinary Research Collaboration (funded by the Engineering and Physical Sciences Research Council) and the European Community under the Integrated Project QAP (funded by the Information Societies Technology directorate as contract no. 015848).

Supporting Online Material

www.sciencemag.org/cgi/content/full/320/5876/638/DC1
Materials and Methods
References

26 December 2007; accepted 12 March 2008
10.1126/science.1154576

Strong Interactions in Multimode Random Lasers

Hakan E. Türeci,[1]* Li Ge,[2] Stefan Rotter,[2]† A. Douglas Stone[2]

Unlike conventional lasers, diffusive random lasers (DRLs) have no resonator to trap light and no high-Q resonances to support lasing. Because of this lack of sharp resonances, the DRL has presented a challenge to conventional laser theory. We present a theory able to treat the DRL rigorously and provide results on the lasing spectra, internal fields, and output intensities of DRLs. Typically DRLs are highly multimode lasers, emitting light at a number of wavelengths. We show that the modal interactions through the gain medium in such lasers are extremely strong and lead to a uniformly spaced frequency spectrum, in agreement with recent experimental observations.

Novel laser systems have emerged recently because of modern nanofabrication capabilities (*1*–*3*). The diffusive random laser (DRL), perhaps the most challenging of the new systems, consists of a random aggregate of particles that scatter light and have gain or are embedded in a background medium with gain (*2*, *4*–*8*). Whereas light scattering in such a random medium can give rise to Anderson-localized, high-Q resonances (*9*, *10*), in almost all experiments the localized regime is not reached, and the laser "cavity" has no isolated resonances in the absence of gain. Despite the lack of sharp resonances, the laser emission from the more recent DRLs (*2*, *5*, *6*) was observed to have the essential properties of conventional lasers: the appearance of coherent emission with line-narrowing above a series of thresholds and uncorrelated photon statistics far from threshold (*11*). Earlier work on random lasers (*4*, *7*) did not find isolated narrow lines and was interpreted as incoherent lasing, in which there was intensity feedback but not amplitude feedback. Later experiments (*2*) and recent numerical studies (*12*) indicated that the lasing involves coherent phase-sensitive feedback in at least some cases. Our work shows that standard coherent multimode lasing is possible even when the linear resonances are much broader than their spacing, raising the question of what determines the emission frequencies of DRLs because they are not determined by the position of passive cavity resonances. Furthermore, recent experiments on porous GaP DRLs have shown that the frequencies are rather uniformly spaced and stable from pulse to pulse, although the intensities vary substantially (*8*). We show that this is a result of strong nonlinear interactions between lasing modes combined with extreme leakiness, a regime particularly difficult to treat. In any multimode laser, the different modes compete with one another through the gain medium in a complex manner that depends on the spatial distribution of the electric field of each mode. This is particularly severe in the DRL, in which there are many spatially overlapping modes with similar (very short) lifetimes.

The finesse, f, of a resonator is defined as the ratio of the resonance spacing to the resonance width; standard laser theory only addresses lasers with high finesse (weakly open) resonators and cannot be applied to the DRL, which has finesse much less than unity. Hence, no analytic results have been derived relating to two-dimensional (2D) or 3D DRLs, and realistic numerical simulations have been limited because of the computational demands. We introduced a formulation of semiclassical laser theory in terms of biorthogonal modes, called constant flux (CF) states, which treats lasing media with any degree of outcoupling and includes the effects of nonlinear modal interactions to all orders (*13*, *14*). We present analytic and numerical results using this approach applied to a DRL.

The simplest model for a laser that captures all of the relevant spatial complexity uses the Maxwell-Bloch equations (*15*, *16*), which are three coupled nonlinear equations for the electric field, the polarization, and the inversion of the gain medium. For stationary multimode lasing, the modes predicted by these equations are determined by the time-independent self-consistent equation (*13*)

$$\Psi_\mu(\boldsymbol{x}) = \frac{i\gamma_\perp}{\gamma_\perp - i(k_\mu - k_a)} \int dx' \frac{D_0(\boldsymbol{x}) G(\boldsymbol{x},\boldsymbol{x}';k_\mu)\Psi_\mu(\boldsymbol{x}')}{\varepsilon(\boldsymbol{x}')\left(1+\sum_\nu \Gamma_\nu |\Psi_\nu(\boldsymbol{x}')|^2\right)} \quad (1)$$

where the electric field is given by $e(\boldsymbol{x},t) = \sum_\mu \Psi_\mu(\boldsymbol{x}) e^{-i\Omega_\mu t}$. In Eq. 1, the lasing frequencies $\Omega_\mu = ck_\mu$ and the lasing mode functions $\Psi_\mu(\boldsymbol{x})$ are assumed to be unknown (henceforth we set the speed of light $c = 1$ and use the wave vector to denote frequency as well). In Eq. 1, k_a is the atomic frequency, $\gamma_\perp$ is the transverse relaxation rate, $\Gamma_\nu = \Gamma(k_\nu)$ is the gain profile evaluated at k_ν, $D_0(\boldsymbol{x}) = D_0\,[1 + d_0(\boldsymbol{x})]$ is the pump, which can vary in space, and $\varepsilon(\boldsymbol{x}) = n^2(\boldsymbol{x})$ is the dielectric function of the "resonator." Electric field and pump strength are dimensionless, being measured in units $e_c = \hbar\sqrt{\gamma_\perp\gamma_\parallel}/2g$ and $D_{0c} = 4\pi k_a^2 g^2/\hbar\gamma_\perp$, where $\gamma_\parallel$ is the longitudinal relaxation rate and g is the dipole matrix element of the gain medium. Each lasing mode Ψ_μ depends nonlinearly on all of the other lasing modes through the denominator in Eq. 1, which represents the "spatial hole-burning" (*15*) interaction with the other modes. Through this mechanism, modes that lase first tend to suppress lasing in other modes, particularly those with which they are correlated in space.

For simplicity we study a 2D DRL and take the gain medium to be a uniform disk of radius R, which contains randomly placed nanoparticles with constant index greater than unity. The light field in the cavity can be either transverse magnetic or transverse electric polarized perpendicular to the plane of the disk, leading to a scalar equation for its normal component. The integral in Eq. 1 is over the gain region, and the kernel $G(\boldsymbol{x},\boldsymbol{x}';k)$ is the Green function of the cavity wave equation with purely outgoing boundary conditions (*13*). This represents the steady-state response of the passive cavity to a monochromatic dipole oscillating with frequency k at $\boldsymbol{x}'$. The nonhermitian boundary conditions on the Green function lead to a spectral representation $G(\boldsymbol{x},\boldsymbol{x}';k)$ in terms of dual sets of biorthogonal functions $\varphi_m(\boldsymbol{x}, k)$ and $\overline{\varphi}_m(\boldsymbol{x}, k)$, termed constant flux (CF) states, with complex eigenvalues, k_m (*13*).

The CF states play the role of the linear cavity resonances within our theory and reduce to the quasi-bound (QB) states within the cavity to a

[1]Institute of Quantum Electronics, Eidgenössische Technische Hochschule (ETH) Zurich, 8093 Zurich, Switzerland. [2]Department of Applied Physics, Post Office Box 208284, Yale University, New Haven, CT 06520–8284, USA.

*To whom correspondence should be addressed. E-mail: tureci@phys.ethz.ch

†Presently on leave from Technische Universitat Wien, Wiedner Hauptstraße 8-10/136, A-1040 Vienna, Austria.

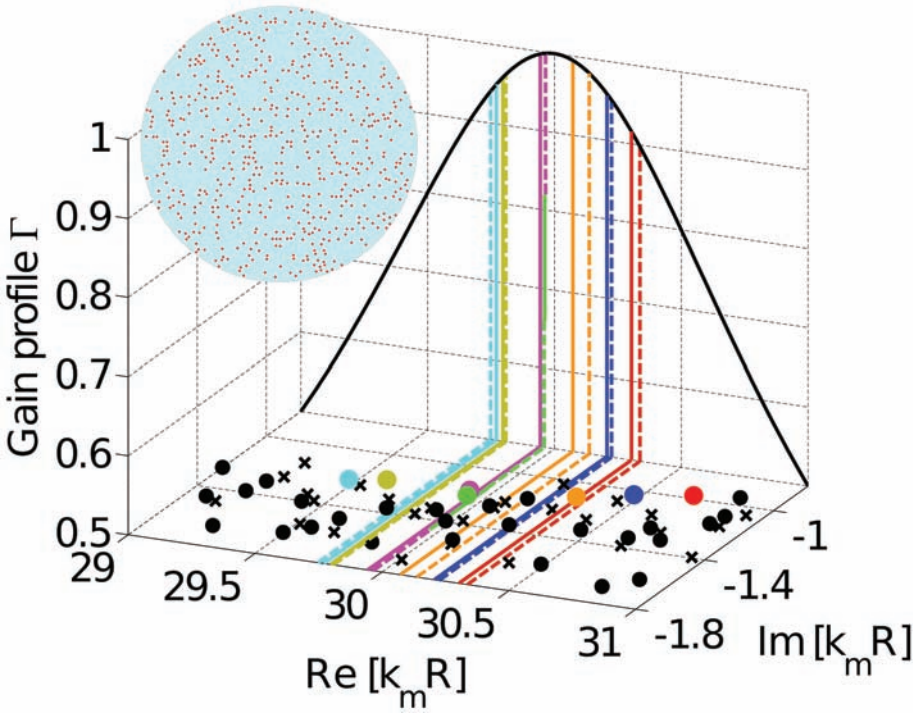

Fig. 1. Lasing frequencies of a DRL. Black circles and crosses represent the complex frequencies of the CF and QB states, respectively; they are distinct but statistically similar. Because their spacing on the real axis is much less than their distance from the axis, the system has no isolated linear resonances, and the cavity has average finesse less than unity ($f \approx 0.05$). Solid colored lines represent the actual frequencies k_μ of the lasing modes at pump $D_0/D_{0c} = 123.5035$; dashed lines denote the values $k_\mu^{(0)}$ arising from the single largest CF state contributing to each mode (the CF frequency is denoted by the corresponding colored circle). The thick black line represents the atomic gain curve $\Gamma(k)$, peaked at the atomic frequency, $k_a R = 30$. Because the cavity is very leaky, the lasing frequencies are strongly pulled to the line center in general; however, the collective contribution to the frequency is random in sign. **(Inset)** Schematic of the configuration of nanoparticle scatterers in the disk-shaped gain region of the DRL.

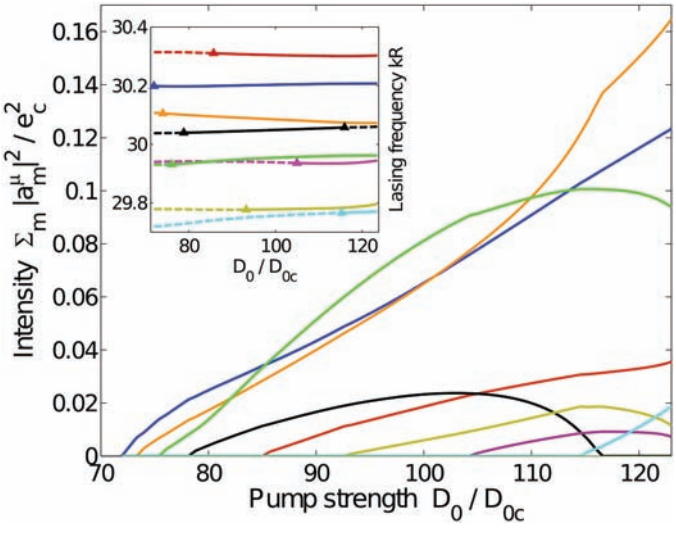

Fig. 2. Lasing intensities of a DRL. Modal intensities of a DRL versus pump D_0 for the disorder configuration of Fig. 1, illustrating complex nonlinear dependence and modal interactions. For example, the black and orange modes approach each other in frequency and interact so strongly that the black mode is driven to zero, at which point the orange mode has a kink in its intensity curve. **(Inset)** The frequencies of each of the eight lasing modes both above (solid) and below (dashed) threshold versus D_0. Note that frequencies can cross if one mode is not lasing but not if both are lasing, and modes with nearby frequencies interact strongly so that their intensity curves are highly anticorrelated. The interactions increase the lasing thresholds substantially. For example, the green and purple modes with $k_\mu \approx 29.95$ have noninteracting thresholds 73.4460 and 75.6919, respectively, but the hole-burning interaction pushes that of the purple mode up to $D_0/D_{0c} \approx 105$. In addition there would be 16 modes lasing by $D_0/D_{0c} = 93$ in the absence of interactions, compared to the 6 we find.

good approximation for a high-Q resonator (*17*). Importantly, the CF states are complete within the cavity and generate a conserved photon flux outside the cavity, unlike the QB states (*13*); for the extremely leaky cavity of a DRL, the CF and QB states are significantly different but statistically similar (Fig. 1).

Because the CF basis is complete and conserves flux outside the gain region, it is an appropriate basis for representing arbitrary lasing modes $\Psi_\mu(\boldsymbol{x})$ of a DRL. To solve Eq. 1, we expand each mode in terms of CF states: $\Psi_\mu(\boldsymbol{x}) = \sum_{m=1}^{N_{CF}} a_m^\mu \varphi_m(\boldsymbol{x})$. Substituting this expansion into Eq. 1 gives an equation for the complex vector of coefficients $\mathbf{a}^\mu = (a_1^\mu, a_2^\mu, \ldots, a_{N_{CF}}^\mu)$ that completely determines Ψ_μ:

$$a_m^\mu = D_0 \sum_n T_{mn}^\mu a_n^\mu \qquad (2)$$

The nonlinear operator T_{mn}^μ is written out explicitly and discussed in (*18*).

This formalism allows us to obtain analytic insight into the question of what determines the frequencies of the DRL. In single-mode lasers, each lasing frequency is a weighted mean of the real part of the cavity resonance frequency and the atomic frequency (*16*), which for a typical high-finesse system is very close to the cavity frequency with a small shift ("pull") toward the atomic line. If we denote the "conventional" lasing frequency by $k_\mu^{(0)}$, we find from Eq. 2 that for the DRL

$$k_\mu \approx k_\mu^{(0)} + k_\mu^{(c)} \qquad (3)$$

where $k_\mu^{(c)}$ is a collective contribution due to all the other CF states, which has no analog in conventional lasers. In our parameter regime ($k_a R \approx 30$), both the conventional and collective terms are important (although the conventional term is larger), and the lasing frequencies have no simple relationship to the cavity frequencies. The collective term is random in sign and does not always generate a pull toward line center (Fig. 1). We believe that at larger $k_a R$ the collective term will dominate.

In Fig. 2, we plot the intensities associated with the lasing modes of Fig. 1 as a function of pump strength, D_0, measured by the length of the vector of CF coefficients, $I = \sum_{m=1}^{N_{CF}} |a_m^\mu|^2$. The behavior is very different from conventional lasers, showing complex nonmonotonic and reentrant behavior in contrast to the linear increase found for uniform edge-emitting lasers (*14*). Analysis reveals that the complex behavior is due to the strong spatial hole-burning interactions in these systems. The Fig. 2 inset shows the lasing frequencies associated with the modes as a function of pump; of the eight lasing modes in the interval, there are six that form three pairs nearby in frequency, and their behavior is highly correlated. Evaluation of the overlap of the $\mathbf{a}^\mu$ vector associated with each pair of modes confirms that not only their frequencies but also their decomposition into CF states are similar.

Equations 1 and 2 imply that modes with similar $\mathbf{a}^\mu$ vectors and similar frequencies will

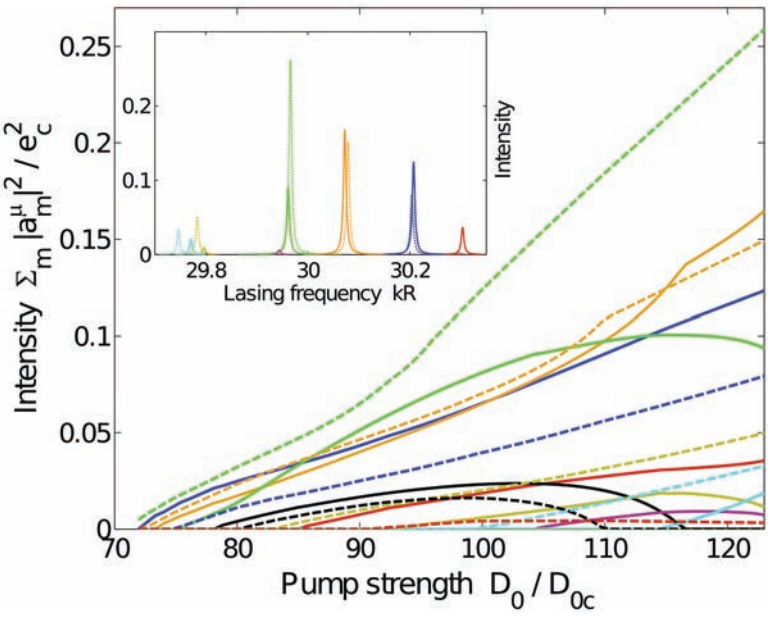

Fig. 3. Intensity and frequency fluctuations in a DRL. Comparison of modal intensities of the DRL for the same disorder configuration in the case of uniform pumping (solid lines) and partially nonuniform pumping (dashed lines). The main source of the large intensity fluctuations is the shift in thresholds. This has the largest effect for nearly degenerate mode pairs such as the green and purple modes ($k_\mu \approx 29.95$). (**Inset**) Lasing spectra at $D_0/D_{0c} = 123.5035$ (lines broadened for visibility). Note that the black mode does not appear at this pump because it has already been suppressed by the orange mode, and the purple mode only appears for uniform pumping because it never reaches threshold in the nonuniform case. The intensities at this pump can fluctuate by more than a factor of two between the two cases, whereas the frequencies fluctuate by just a few percent of their average spacing.

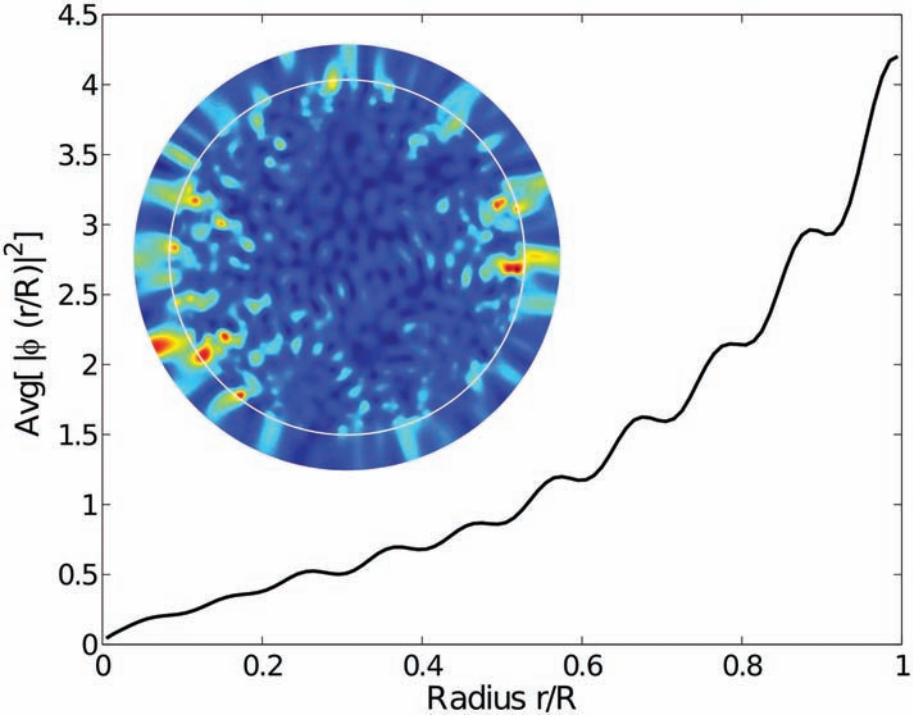

Fig. 4. Field distribution of a DRL. Radial intensity of CF states contributing to the lasing modes averaged over 400 disorder configurations. There is a large nonrandom increase of intensity with radius r. (**Inset**) False color plot of electric field intensity of the seven lasing modes of the DRL of Fig. 1 at pump $D_0/D_{0c} = 123.5035$ (white circle is boundary of gain medium). Note brightest regions appear at the edge of the gain medium; this is characteristic of low finesse lasers but is a particularly large effect in the DRL.

compete strongly because this leads to a hole-burning denominator that is spatially correlated with the numerator. However, it is not obvious that frequency quasi-degeneracy should be associated with spatial correlation for the DRL. For random lasers with Anderson localization (*9*, *10*), the CF states would typically be spatially disjoint, the $T_{mn}(k)$ operator (compare with Eq. S3) would be approximately diagonal, and there would be no such spatial correlation. In additional calculations not shown, we do find that for larger index nanoparticles, which begin to localize the CF states, the modal interactions are reduced. But for the DRL, $T_{mn}(k)$ is not diagonal, and frequency degeneracy would require an eigenvalue degeneracy in this complex pseudo-random matrix [see discussion in (*18*)]. Instead, there is eigenvalue repulsion in the complex plane and strong mixing of eigenvectors, resulting in large spatial overlap of quasi-degenerate lasing modes and strong hole-burning interaction. This interaction, in the absence of some special symmetry, tends to suppress one of the two modes, leading to well-spaced lasing frequencies as found by (*8*). Hence, the rigid lasing-frequency spectrum could distinguish the DRL from an Anderson-localized laser.

This strong interaction of nearly degenerate modes is reflected in a very large increase in the lasing threshold of the second mode of each pair (Fig. 2 caption) (*18*). These interaction effects are strongly nonlinear and hence highly sensitive to statistical fluctuations. To illustrate this, in Fig. 3 we contrast the intensity behavior of Fig. 2, for which the pump was uniform in space [$d_0(\boldsymbol{x}) = 0$], with a case for which we have added to the uniform pump a random white noise term $d_0(\boldsymbol{x})$ of standard deviation ±30% (normalized to the same total power). For this nonuniform pump, the third uniform mode (green) now turns on first. It is thus able to suppress the seventh uniform mode (purple) over the entire range of pump powers and acquires an intensity almost a factor of 3 greater at the same average pump power. The intensities of all the interacting pairs show similar high sensitivity to pump profile, whereas their frequencies remain relatively stable (Fig. 3 inset). Exactly such behavior was observed in shot-to-shot spectra of DRLs in experiments (*8*).

Lastly, we consider the spatial variation of the electric field in DRLs (Fig. 4). The false-color representation of the multimode electric field in the laser has a striking property: It is consistently brighter at the edge of the disk than at its center, even though the gain is uniform and there are no special high-Q modes localized near the edge. To demonstrate that this effect is not a statistical fluctuation associated with this particular disorder configuration, we have averaged the behavior of the entire basis set of CF states over disorder configurations. The result is a nonrandom average growth of intensity toward the boundary. The origin of this effect is known from earlier work on distributed feedback lasers with weak reflectivity (*19*); if the single-pass loss is large,

then the single-pass gain must also be large in order to lase, leading to a visible nonuniformity of the lasing mode, with growth in the direction of the loss boundary (on average the radial direction for the DRL). Because the DRL has fractional finesse (which is not achievable in a 1D geometry), this effect is much larger in these systems and should be observable. This effect means that the electric field fluctuations in DRLs will differ substantially from the random matrix/quantum chaos fluctuations of linear cavity modes (*20*), first because each mode is a superposition of pseudo-random CF states and second because these CF states themselves are not uniform on average.

The coexistence of gain, nonlinear interactions, and overlapping resonances (fractional finesse) makes the DRL a more complex and richer system than the widely studied linear wave-chaotic systems. It remains to be seen whether concepts from random matrix theory and semiclassical quantum mechanics (quantum chaos) will prove fruitful in this context. The theory presented here is ab initio in the sense that it generates all properties of the lasing states from knowledge of the dielectric function of the host medium and basic parameters of the gain medium; it should be applicable to any novel laser-cavity system.

References and Notes

1. K. J. Vahala, *Nature* **424**, 839 (2003).
2. H. Cao, *J. Phys. A* **38**, 10497 (2005).
3. O. Painter *et al*., *Science* **284**, 1819 (1999).
4. N. M. Lawandy, R. M. Balachandran, A. S. L. Gomes, E. Sauvain, *Nature* **368**, 436 (1994).
5. S. Mujumdar, M. Ricci, R. Torre, D. S. Wiersma, *Phys. Rev. Lett.* **93**, 053903 (2004).
6. H. Cao *et al*., *Phys. Rev. Lett.* **82**, 2278 (1999).
7. H. Cao, *Waves Random Media* **13**, R1 (2003).
8. K. L. van der Molen, R. W. Tjerkstra, A. P. Mosk, A. Lagendijk, *Phys. Rev. Lett.* **98**, 143901 (2007).
9. P. Pradhan, N. Kumar, *Phys. Rev. B* **50**, 9644 (1994).
10. V. Milner, A. Z. Genack, *Phys. Rev. Lett.* **94**, 073901 (2005).
11. H. Cao, Y. Ling, J. Y. Xu, C. Q. Cao, P. Kumar, *Phys. Rev. Lett.* **86**, 4524 (2001).
12. C. Vanneste, P. Sebbah, H. Cao, *Phys. Rev. Lett.* **98**, 143902 (2007).
13. H. E. Türeci, A. D. Stone, B. Collier, *Phys. Rev. A* **74**, 043822 (2006).
14. H. E. Türeci, A. D. Stone, L. Ge, *Phys. Rev. A* **76**, 013813 (2007).
15. H. Haken, H. Sauermann, *Z. Phys.* **173**, 261 (1963).
16. H. Haken, *Light: Laser Dynamics* (North-Holland, Amsterdam, 1985), vol. 2.
17. In a high-finesse cavity, QB and CF states are essentially the same, each lasing mode is associated with one QB state, and the lasing frequency takes the value $k_\mu^{(0)}$ between the atomic line center and the cavity frequency q_1 determined by the ratio of $\gamma_\perp/\kappa$ (*13*).
18. Materials and methods are available on *Science* Online.
19. H. Kogelnik, C. V. Shank, *J. Appl. Phys.* **43**, 2327 (1972).
20. A. Kudrolli, S. Sridhar, A. Pandey, R. Ramaswamy, *Phys. Rev. E* **49**, R11 (1994).

21. This work was supported by NSF grant DMR-0408636, by the Max Kade and W. M. Keck foundations, and by the Aspen Center for Physics. We thank R. Tandy, M. Machida, H. Cao, A. Lagendijk, P. Sebbah, C. Vanneste, and D. Wiersma for discussions.

Supporting Online Material

www.sciencemag.org/cgi/content/full/320/5876/643/DC1
Materials and Methods
Figs. S1 to S3
References and Notes

16 January 2008; accepted 25 March 2008
10.1126/science.1155311

Silica-on-Silicon Waveguide Quantum Circuits

Alberto Politi, Martin J. Cryan, John G. Rarity, Siyuan Yu, Jeremy L. O'Brien*

Quantum technologies based on photons will likely require an integrated optics architecture for improved performance, miniaturization, and scalability. We demonstrate high-fidelity silica-on-silicon integrated optical realizations of key quantum photonic circuits, including two-photon quantum interference with a visibility of 94.8 ± 0.5%; a controlled-NOT gate with an average logical basis fidelity of 94.3 ± 0.2%; and a path-entangled state of two photons with fidelity of >92%. These results show that it is possible to directly "write" sophisticated photonic quantum circuits onto a silicon chip, which will be of benefit to future quantum technologies based on photons, including information processing, communication, metrology, and lithography, as well as the fundamental science of quantum optics.

Quantum information science (*1*) has shown that quantum mechanical effects can dramatically improve performance for certain tasks in communication, computation, and measurement. Of the various physical systems being pursued, single particles of light (photons) have been widely used in quantum communication (*2*), quantum metrology (*3*–*5*), and quantum lithography (*6*) settings. Low noise (or decoherence) also makes photons attractive quantum bits (or qubits), and they have emerged as a leading approach to quantum information processing (*7*).

In addition to single-photon sources (*8*) and detectors (*9*), photonic quantum technologies require sophisticated optical circuits involving high-visibility classical and quantum interference. Although a number of photonic quantum circuits have been realized for quantum metrology (*3*, *4*, *10*–*13*), lithography (*6*), quantum logic gates (*14*–*20*), and other entangling circuits (*21*–*23*), these demonstrations have relied on large-scale (bulk) optical elements bolted to large optical tables, thereby making them inherently unscalable.

We demonstrate photonic quantum circuits using silica waveguides on a silicon chip. The monolithic nature of these devices means that the correct phase can be stably realized in what would otherwise be an unstable interferometer, greatly simplifying the task of implementing sophisticated photonic quantum circuits. We fabricated hundreds of devices on a single wafer and find that performance across the devices is robust, repeatable, and well understood.

A typical photonic quantum circuit takes several optical paths or modes (some with photons, some without) and mixes them together in a linear optical network, which in general consists of nested classical and quantum interferometers (e.g., Fig. 1C). In a standard optical implementation, the photons propagate in air, and the circuit is constructed from mirrors and beam splitters (BSs), or half-reflective mirrors, which split and recombine optical modes, giving rise to both classical and quantum interference. High-visibility quantum interference (*24*) demands excellent optical mode overlap at a BS, which requires exact alignment of the modes, whereas high visibility classical interference also requires subwavelength stability of optical path lengths, which often necessitates the design and implementation of sophisticated stable interferometers. Combined with photon loss, interference visibility is the major contributor to optical quantum circuit performance.

In conventional (or classical) integrated optics devices, light is guided in waveguides—consisting of a core and slightly lower refractive index cladding (analogous to an optical fiber)—which are usually fabricated on a semiconductor chip. By careful choice of core and cladding dimensions and refractive index difference, it is possible to design such waveguides to support only a single transverse mode for a given wavelength range. Coupling between waveguides, to realize BS-like operation, can be achieved when two waveguides are brought sufficiently close together that the evanescent fields overlap; this is known as a directional coupler. By lithographically tuning the separation between the waveguides and the length of the coupler, the amount of light coupling from one waveguide into the other (the coupling ratio $1 - \eta$, where η is equivalent to BS reflectivity) can be tuned.

The most promising approach to photonic quantum circuits for practical technologies appears to be realizing integrated optics devices that operate at the single-photon level. Key require-

Centre for Quantum Photonics, H. H. Wills Physics Laboratory and Department of Electrical and Electronic Engineering, University of Bristol, Merchant Venturers Building, Woodland Road, Bristol BS8 1UB, UK.

*To whom correspondence should be addressed. E-mail: Jeremy.OBrien@bristol.ac.uk